

## Supporting information

### **Synchronous Dual Additive to Boost Multiphase Interface Stability of High-voltage Li-rich Mn-based batteries**

*Qiangfeng Zhang, Shijie Xu, Haipeng Zhu, Zhao Chen, Libao Chen, Chunxiao*

*Zhang\*, and Weifeng Wei*

State Key Laboratory of Powder Metallurgy, Central South University, Changsha,  
Hunan, 410083, P. R. China.

E-mail: [chunxiaozhang@csu.edu.cn](mailto:chunxiaozhang@csu.edu.cn) (C. Zhang)

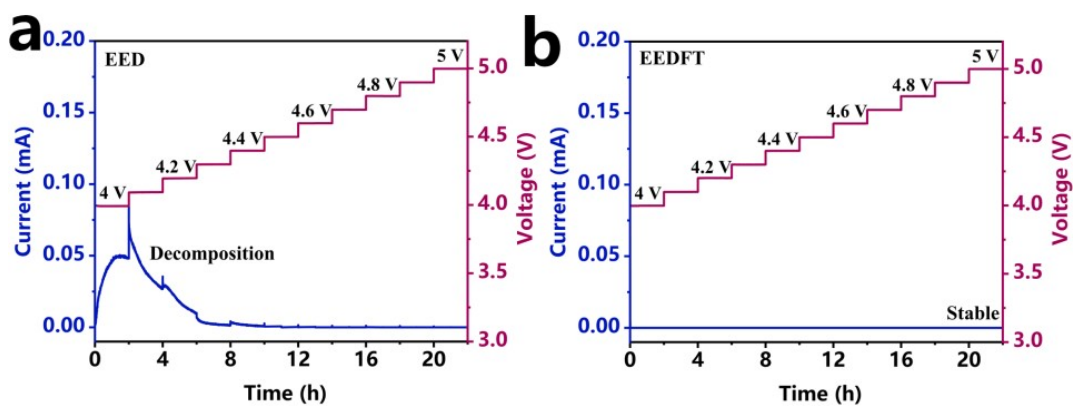


Figure S1. Potentiostatic polarization of Li||Al cells with (a) EED and (b) EEDFT.

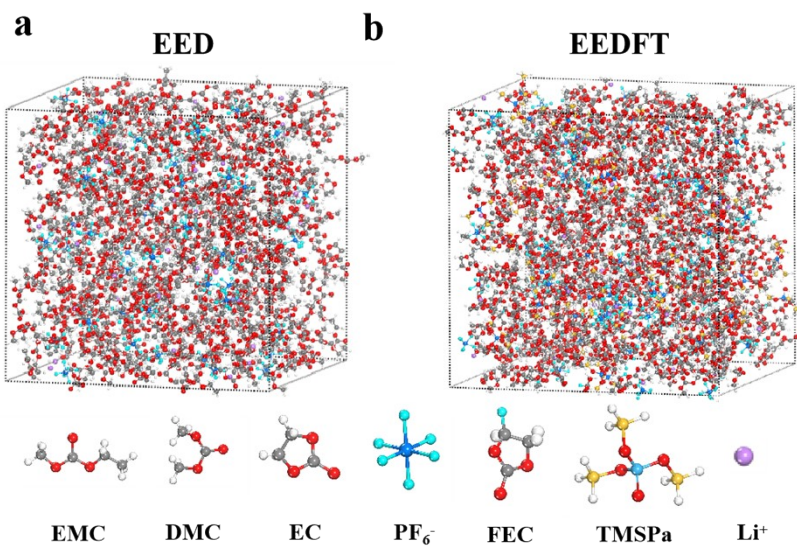


Figure S2. MD simulation snapshots of EED (a) and EEDFT(b)electrolytes.

Table S1. The values of the coordination number in various electrolytes.

Coordination number	EC	EMC	DMC	PF <sub>6</sub> <sup>-</sup>
EED	1.04	1.56	2.00	0.79
EEDFT	0.90	1.17	1.83	0.62

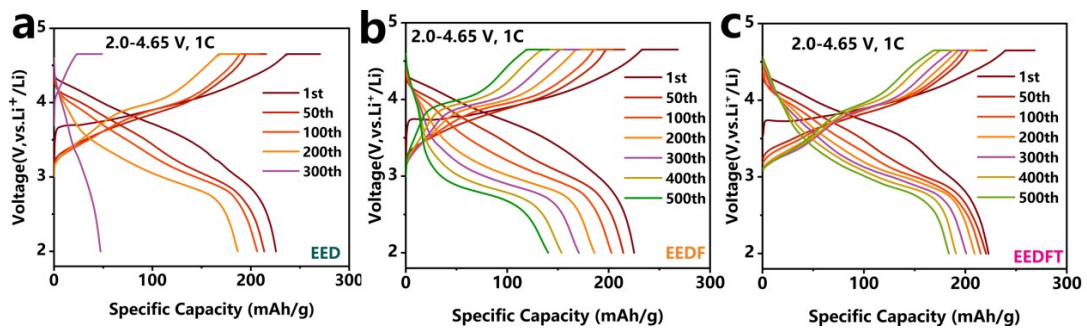


Figure S3. Charge-discharge curves of different cycles using EED electrolyte (a); EEDF electrolyte (b) and EEDFT electrolyte (c).

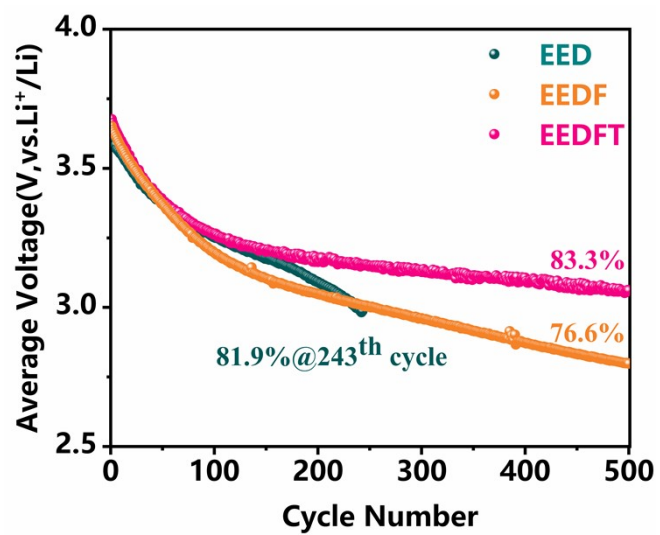


Figure S4. Voltage decay during the cycle at 1 C

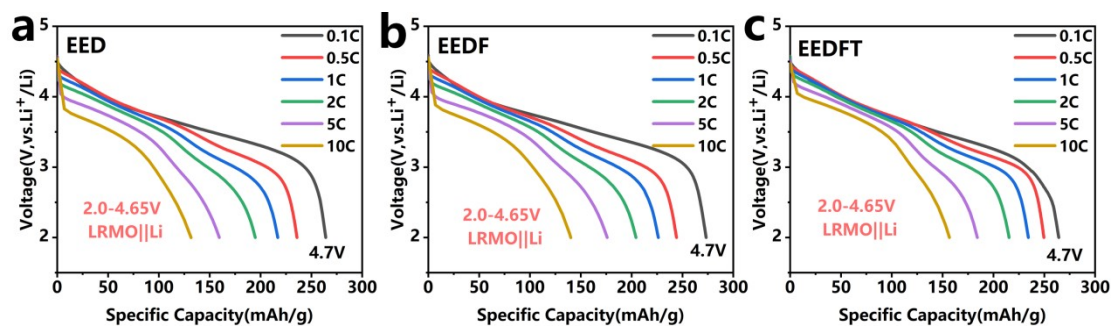


Figure S5. Discharge curves of different current density at 0.1 C-10 C using EED electrolyte (a); EEDF electrolyte (b) and EEDFT electrolyte (c).

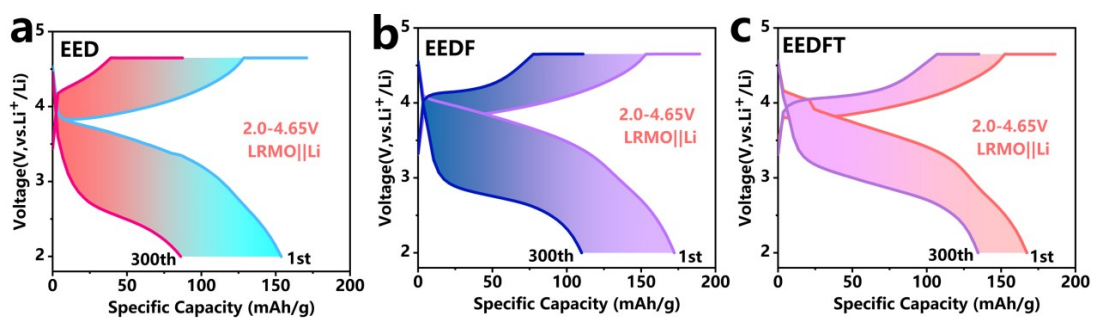


Figure S6. Charge-discharge curves at the high current density of 5 C during cycling using EED electrolyte (a); EEDF electrolyte (b) and EEDFT electrolyte (c).



Table S2. Comparison of the electrochemistry performances of the GPE electrolyte with reported results.

No.	Electrolyte system	Rate	Cycles	Capacity retention	Ref.
1	EC/DMC/DEC+FEC	0.5 C	100	93.85%	[1]
2	EC/DMC+LiBOB	0.1 C	50	98%	[2]
3	EC/DMC+LiPO <sub>2</sub> F <sub>2</sub>	3 C	500	85%	[3]
4	EC/DMC/EMC+LiDFOB+TMSPi	1 C	300	87.7%	[4]
5	EC/DMC/EMC+LiDFOB+THFPB	1 C	200	92.19%	[5]
6	EC/DEC+HTCN+TMSP	1 C	200	93.83%	[6]
7	EC/EMC/DMC+CFBA	0.5 C	200	88.4%	[7]
8	EC/DMC+TPFPB	1/3 C	500	76.8%	[8]
9	This work	1 C	500	82.36%	
10	This work	5 C	300	80.4%	

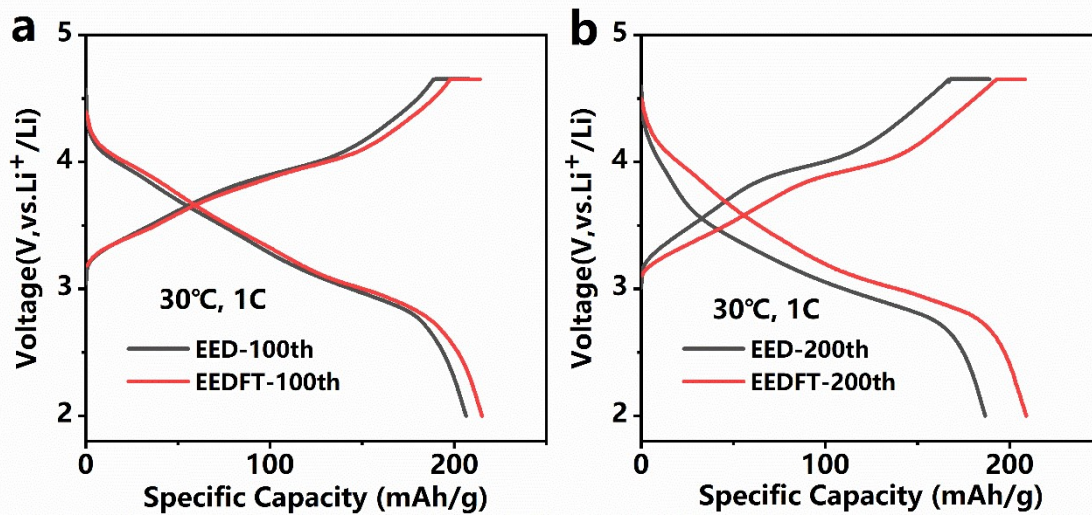


Figure S7. Charge-discharge curves from the 100th (a) to the 200th (b) cycle at 30°C.



Figure S8. Diffraction fringes obtained by the corresponding inverse Fourier transform in region II.

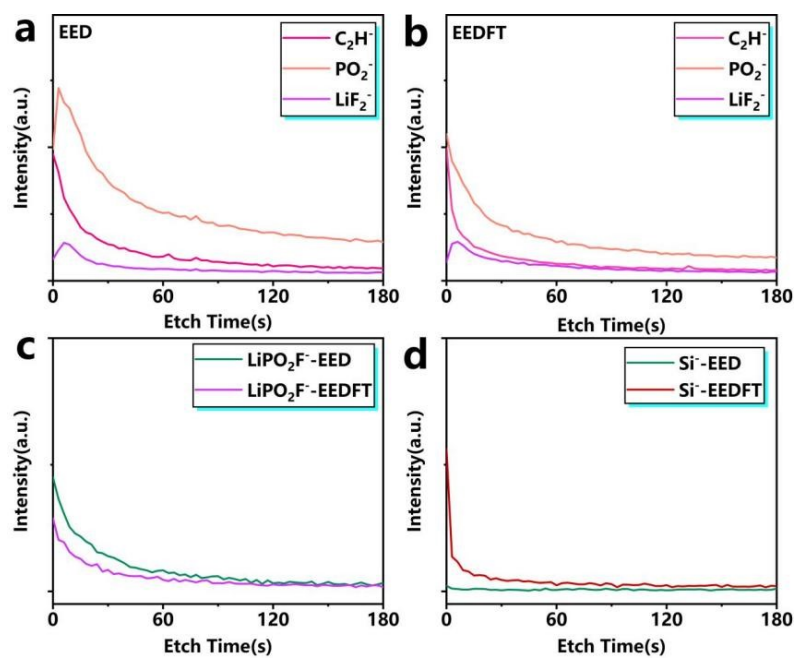


Figure S9. Sputtering profiles of LRMO cathodes with EED electrolyte(a); EEDFT electrolyte (b);  $\text{LiPO}_2\text{F}^-$ (c) and  $\text{Si}^-$ (d) obtained by ToF-SIMS

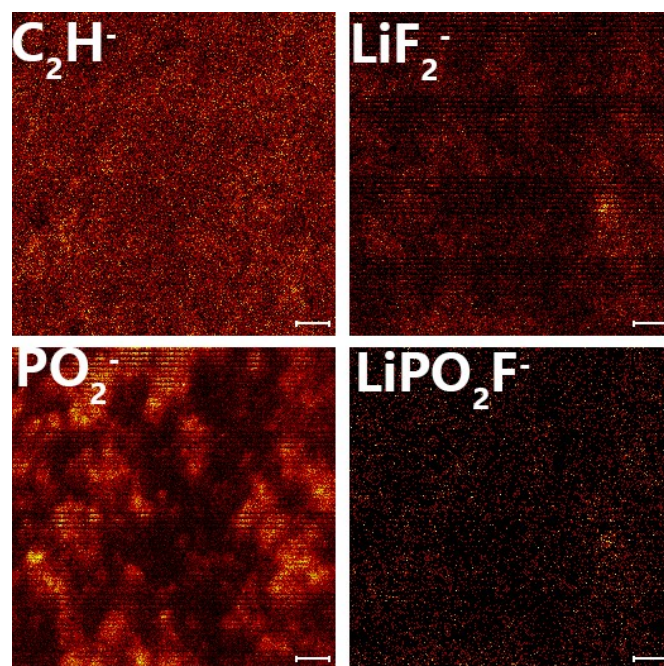


Figure S10. 2D view of LRMO cathodes with EED electrolyte obtained by ToF-SIMS

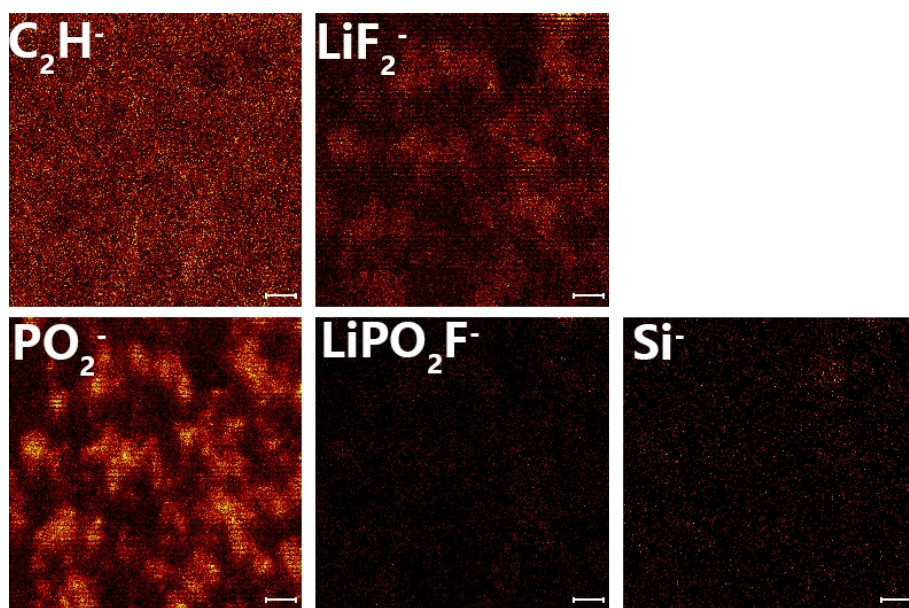


Figure S11. 2D view of LRMO cathodes with EEDFT electrolyte obtained by ToF-SIMS

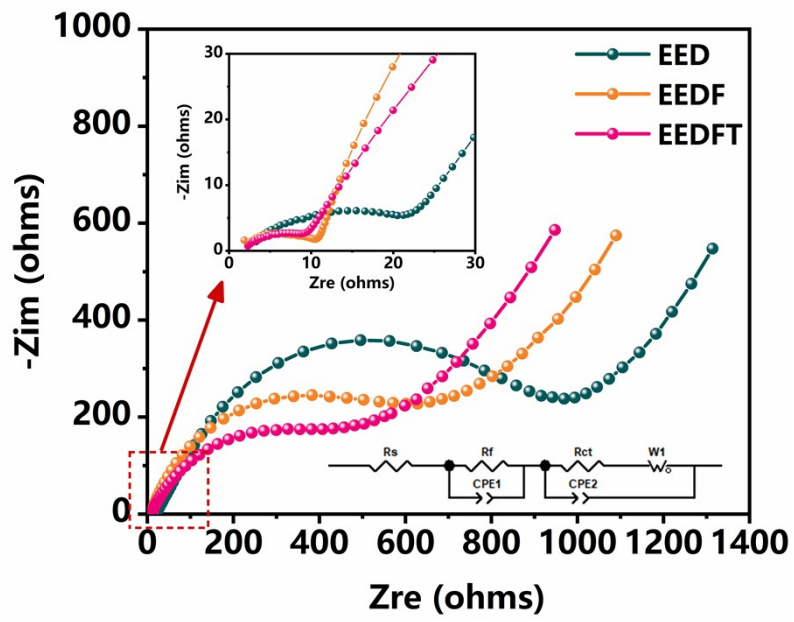


Figure S12. EIS plots of LRMO||Li cells after 30 cycles using various electrolytes.

Table S3.  $R_f$  and  $R_{ct}$  of LRMO||Li cells with different electrolytes after cycled.

Values of $R_f$ and $R_{ct}$	EED	EEDF	EEDFT
$R_f(\Omega)$	21.6	9.4	7.4
$R_{ct}(\Omega)$	1032	439.3	368.5



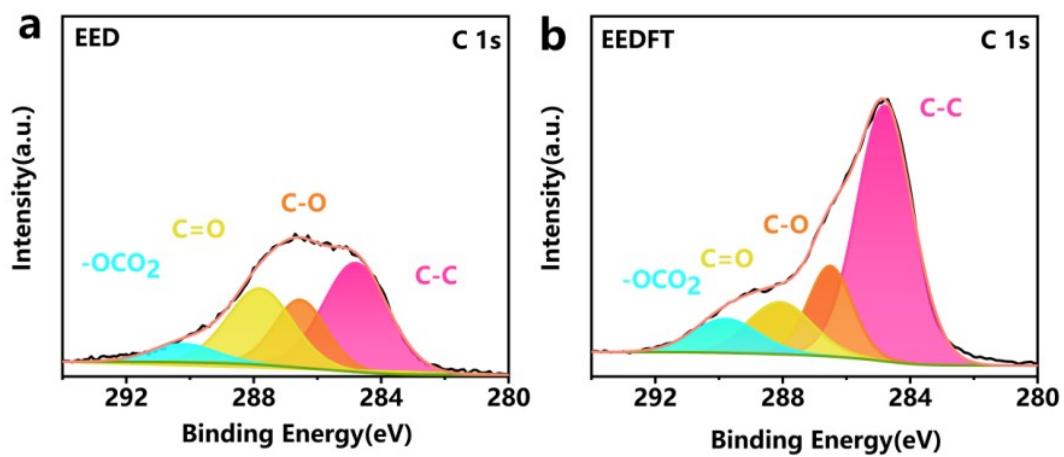


Figure S13. C 1s XPS spectra of the SEI formed on the lithium metal anode after 100 cycles in the LRMO||Li cells with EED (a) and EEDFT (b).

## References:

1. Y. Li, F. Lian, L. Ma, C. Liu, L. Yang, X. Sun and K. Chou, *Electrochimica Acta*, 2015, **168**, 261-270.
2. P. K. Nayak, J. Grinblat, M. Levi and D. Aurbach, *Journal of The Electrochemical Society*, 2015, **162**, A596.
3. B. Jiang, J. Li, B. Luo, Q. Yan, H. Li, L. Liu, L. Chu, Y. Li, Q. Zhang and M. Li, *Journal of Energy Chemistry*, 2021, **60**, 564-571.
4. Z. Lu, D. Liu, K. Dai, K. Liu, C. Jing, W. He, W. Wang, C. Zhang and W. Wei, *Energy Storage Materials*, 2023, **57**, 316-325.
5. K. Ma, Y. Cao, S. Zhang, Y. Zhang, S. Fang, X. Han, F. Jin and J. Sun, *Nano Letters*, 2024, **24**, 8826-8833.
6. J. Zhao, Y. Liang, X. Zhang, Z. Zhang, E. Wang, S. He, B. Wang, Z. Han, J. Lu, K. Amine and H. Yu, *Advanced Functional Materials*, 2021, **31**, 2009192.
7. S. Gu, Y. Cui, K. Wen, S. Chen and J. Zhao, *Journal of Alloys and Compounds*, 2020, **829**, 154491.
8. J. Zheng, J. Xiao, M. Gu, P. Zuo, C. Wang and J.-G. Zhang, *Journal of Power Sources*, 2014, **250**, 313-318.